SIMPLE VIEWS ON CORNERED CONTACT LINES NEAR INSTABILITY

J.H. Snoeijer and I. Peters
Physics of Fluids Group
University of Twente
P.O. Box 217, 7500 AE
Enschede, The Netherlands
Email: j.h.snoeijer@tnw.utwente.nl

L. Limat and A. Daerr
Laboratoire Matière et Systèmes Complexes
UMR CNRS 7057, Université Paris Diderot
10 rue Alice Domon et Léonie Duquet
75205 Paris cedex 13, France
laurent.limat@univ-paris-diderot.fr

ABSTRACT

Drops sliding down a partially wetting plate develop a sharp, cornered tail that above a critical speed emits little droplets. Similar contact line shapes and instabilities appear in coating and splashing and owing to the three-dimensional corner geometry the flow requires complicated modeling. Here we propose a simple comprehensive view of recent theoretical efforts, which describe these phenomena using the lubrication approximation. In particular, we derive explicit formulas for the opening angle of the corner and the curvature at the tip as a function of drop velocity. We present a detailed comparison of the model predictions with experimental results, confirming the strength of lubrication-based models to describe wetting phenomena, even for complicated geometries.

INTRODUCTION

Coating techniques are most often faced with partial wetting conditions. When pulled out of a bath at moderate speed, a tape or a plate entrains a film of triangular shape, edged by two oblique contact lines meeting in a singular point [1]. This effect, and its equivalent for plunging tapes (entrainment of triangular air pockets), limits the efficiency of coating [2,3]. Recent progress has been made on these phenomena by combining experiments on drops sliding down a plane [4-5,9] and lubrication models [6-9], but the description remains very complex. In the present paper we show that a simple modeling is sufficient to give reasonable predictions of both the opening angle of the corner, and of the typical radius of curvature that limits the singularity at the corner tip. We compare these predictions to experiments performed on silicon oil drops sliding down a inclined plate.

EXPERIMENTS

In our experiment [4-9], trains of silicon oil drops of constant volume are left sliding along inclined glass plates coated with a fluoropolymer (FC725 from 3M) that forces partial wetting conditions, with typical advancing and receding contact angles of order $\theta_a = 50°$, and $\theta_r = 45°$. Different viscosities η ranging between 10 and 1000 cP were explored, while keeping the liquid mass density ($\rho \approx 0.93$ to 0.97 gr/cm^3) and its surface tension ($\gamma \approx 20$ to 21 mN/m) nearly constant. All these experiments gave the same results, provided that one plots any quantity as a function of the capillary number $\mathrm{Ca} = \eta U/\gamma$, built upon the drop velocity U controlled by selecting the tilt angle of the plane. At low Ca, the drops remain rounded, but develop a "corner singularity" at their rear front when Ca exceeds a critical value of order 0.004, and undergo a "pearling transition" above another critical Ca of order 0.007. Typical pictures are reproduced on Fig.1 and Fig.2. As appears on Fig.1a, the cornered contact line is in fact associated to a conical interface described by two distinct angles: the corner opening half angle ϕ and the angle viewed from the side Ω. This conical singularity is regularized at small scale (Fig. 1b) by a strongly curved portion of contact line of typical radius of curvature $R = 1/\kappa$, of order 20 to 100 μm. The three quantities ϕ, Ω, R are decreasing functions of Ca, which will be specified in the next section.

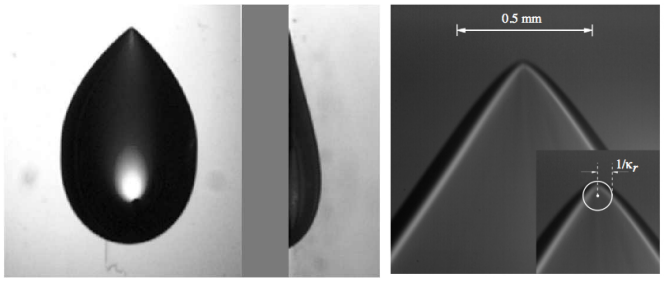

Fig.1: Left: "Cornered" silicon oil drop sliding down an incline, with both a view from the top and a view from the side. Motion is from the top to the bottom of the figure. Right: Magnified view of the corner tip, regularized at a scale $R = 1/\kappa$ by a strongly curved contact line

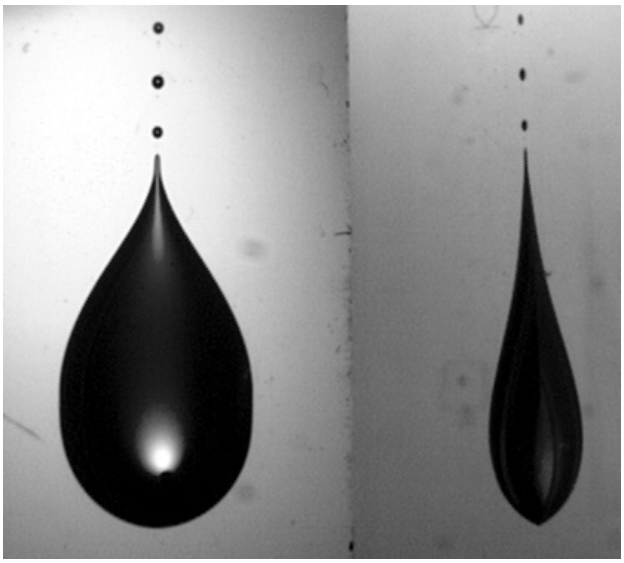

Fig.2: Top view and side view from a drop above the "pearling transition". At high enough sliding velocities the receding contact line becomes unstable and emits small droplets from the sharp tip.

SIMPLE MODELING OF ϕ AND R

In the limit of low opening angle ϕ, the liquid thickness (Fig.3, left) can be approximated [6] as:

$$h(x,y) = \Omega x \left[1 - \frac{y^2}{x^2 \tan^2 \phi}\right]. \qquad (1)$$

In the drop framework the liquid flux entrained by the substrate towards the corner tip $J = Uh(x)$ balances that expulsed by capillarity in the opposite direction $J = -(h^3/3\eta)dP/dx$, where $P = -\gamma\Delta h(x,y)$ is the capillary pressure. Calculating both fluxes on the central axis yields:

$$\Omega^3 = m\mathrm{Ca}\tan^2\phi, \qquad (2)$$

with $m = 3/2$ in this simple approach [6]. A better accuracy is obtained by averaging the flux on the whole parabolic cross-section [7], rather than working only close to $y = 0$, and yields $m = 35/16$. A second relationship is obtained by assuming that this cone structure has to match the usual Cox-Voinov description of dynamics on the two oblique contact lines [8], at some macroscopic scale L:

$$\theta^3 \approx \left(\frac{2\Omega}{\sin\phi}\right)^3 \approx \theta_r^3 - 9\mathrm{Ca}\sin\phi\ln(L/l), \qquad (3)$$

where l is the microscopic scale at which one recovers the equilibrium contact angle, or at least the static receding contact angle θ_r. Note here that: (i) Ca has been replaced by the effective capillary number $\mathrm{Ca}\sin\phi$, built upon the normal velocity $U\sin\phi$ that coincides with the true fluid velocity at the approach of contact lines [7], and (ii) this matching is not perfect as it can not be valid uniformly at any scale over the whole oblique contact lines.

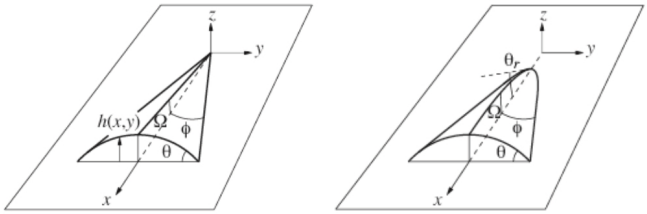

Fig.3: Modeling the corner tip as a perfect cone (left) and as a cone rounded at a small scale (right).

One can eliminate Ω from these two equations and yields in the low ϕ limit the following selection of ϕ with Ca:

$$\frac{\mathrm{Ca}}{\theta^3} = \frac{2\sin\phi}{18\sin^2\phi\ln(L/l) + 35/\cos^2\phi} \approx \frac{2\phi}{18\phi^2\ln(L/l) + 35}. \qquad (4)$$

This relationship is compared to our experimental data obtained on sliding drops, in Fig. 4. The agreement is not so bad considering the rough approximations underlying (3). The crucial original feature of (4) is the prediction a critical Ca above which the corner can not exist. We conjecture that this critical point corresponds to the pearling transition at which the data disappear. The critical opening angle related to this transition $\phi_c \approx 25°$ is in rather good agreement with that observed experimentally ($\phi_c \approx 30°$) [5-7]. Omitting the factor 35 in (4), one recovers the result by Podgorski et al. [4] expressing the hypothesis of Blake and Ruschak that the two oblique contact lines remain just at the limit of the forced wetting transition [1]. This idea, however, does not lead to a pearling transition and seems clearly ruled out by our data. In hindsight, this means that the two oblique contact lines can not be treated as independent [9], which was implicitly assumed in refs.[1,4].

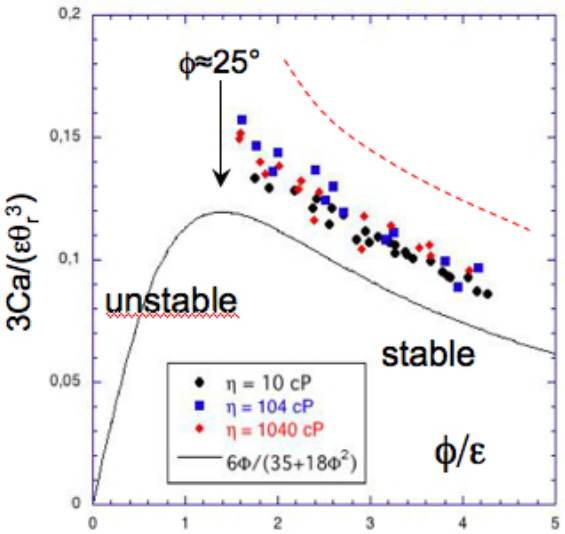

Fig.4: Relationship (4) linking the corner angle ϕ to the dimensionless drop velocity Ca (solid line), compared to experiments for different values of the viscosity (symbols). The angle ϕ is in radians and $\epsilon = 1/[Log(b/a)]^{1/2} \approx 0.3$ is deduced from dynamic contact angle measurements on oval drops. The solid line displays a maximum Ca, which is interpreted as the onset of the pearling instability. We also

plot the model by Podgorski (dotted line), which does not display a maximum speed.

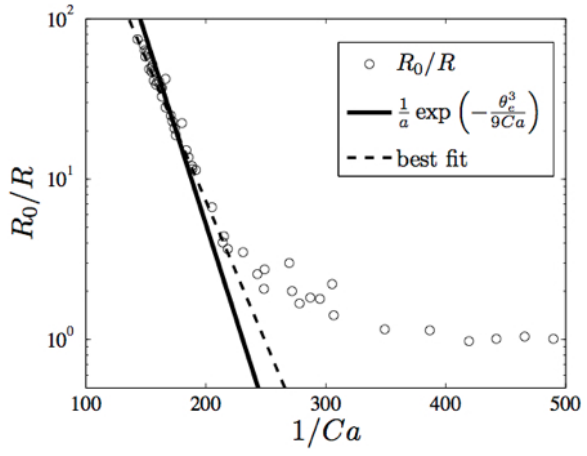

Fig.5: Tip radius R versus Ca, measured for 20 cP oil ($\eta = 19.6$ cP, $\rho = 940$ Kg/m^3, γ=20.5 mN/m), and compared to the lubrication prediction (7) with $\theta_e = \theta_r$ (continuous line) and θ_e as adjustable free parameter (dashed line). $R_0 = 1.63$ mm represents the initial radius of of curvature of the contact line at zero speed.

A similar approach can be followed to describe the radius of curvature R at the tip of the corner, still in the limit of low ϕ (fig. 3, right). The idea is now to combine the parabolic cross section of the corner tip to contact line of hyperbolic shape [9]. The contour of the contact line at the rear of the drop is then described by $y_{\rm cl}^2 = 2Rx + \phi^2 x^2$. This form indeed has a tip radius R, and reduces to the perfectly sharp corner as $R \to 0$. We replace this contour in (1) as:

$$h(x,y) = \Omega x \left[1 - \frac{y^2}{2Rx + x^2\phi^2}\right]. \qquad (5)$$

At small scale $x \ll R$, this structure should match to a contact line of negligible curvature and tangent to Oy, for which we expect a Cox-Voinov behavior of the slope. This crosses over to the cone angle Ω at a length scale of order $2R/\phi^2$, which finally implies that:

$$\Omega^3 \approx \theta_r^3 - 9\mathrm{Ca}\ln\left(\frac{2R}{l\phi^2}\right). \qquad (6)$$

For a more rigorous derivation of this result we refer to [9]. Note that choosing a contact line shape different from the hyperbolic fit will only affect the constant inside the logarithm of this equation. Combined with the other equations yields approximately for high enough Ca:

$$R \approx \frac{l\phi^2}{2}\exp\left(\frac{\theta_e^3}{9\mathrm{Ca}}\right). \qquad (7)$$

Here, the prefactor $a = l\phi^2/2$ varies much slowly than the exponential factor and $\theta_e = \theta_r$.

We have plotted measurements of $1/R$ versus $1/\mathrm{Ca}$ on fig.5. On the same plot we compare these data with the prediction (7). The observed fit is quite good and yields an estimate of the microscopic prefactor a of order 10 nm, consistent with the typical size a of molecules (a few nanometers in [4]). A better fit is even possible, letting θ_e free to adjust itself to another microscopic value ($\theta_e = 41^\circ$ with $a = 65$ nm). This suggests that though we have used Cox-Voinov description of contact lines [10], our work is not incompatible with more refined theories of wetting dynamics at microscopic scale [11].

CONCLUSIONS

In this short paper we reviewed recent progress on the lubrication description of cornered contact lines, yielding explicit predictions for the geometry of the corner as a function of sliding speed. The comparison with experimental results confirms that such models are very effective, even when the vicinity of the contact line displays a fully three-dimensional interface structure. It is interesting to note that similar dewetting corners appear naturally in the context of Immersion Lithography. This is a technique that is currently applied in semiconductor industry to achieve higher optical resolutions, and accordingly smaller dimensions [12,13]. The resolution of the conventional Lithography method, which consists of the projection of light patterns through a lens on substrates, is improved by replacing the air between the lens and the substrate by a liquid with a higher refractive index. It was recently found that cornered contact lines in Immersion Lithography systems display very similar behavior as the sliding drops [14]. Note, however, that both the liquid and way the contact line is forced to move over the solid is completely different in comparison to the sliding drops. This illustrates that the validity of the lubrication models for dewetting corners is very general and certainly goes beyond the experiments discussed in the present paper.

ACKNOWLEDGMENTS

We are indebted to collaborations with J. Eggers, H.-A. Stone, N. le Grand-Piteira and E. Rio.

REFERENCES

[1] Blake, T.D., Ruschak, K.J. 1979, Nature 282, 489.
[2] Burley, R., Kennedy, B.S. 1976, Chem. Eng. Sci. 31, 901.
[3] Benkreira, H., Khan, M.I. 2008, Chem. Eng. Sci. 63, 448.
[4] Podgorski, T., Flesselles, J.-M., Limat, L. 2001, Phys. Rev. Lett. 87, 036102.
[5] Le Grand, N., Daerr, A., Limat, L. 2005, J. Fluid Mech. 541, 293.
[6] Limat, L., Stone, H.A. 2003, Europhys. Lett. 65, 365.
[7] Snoeijer, J.H., Rio, E., Le Grand, N., Limat L. 2005, Phys. Fluids 17, 072101.
[8] Snoeijer, J.H., Le Grand-Piteira, N., Limat L., Stone, H.A., Eggers, J. 2007, Phys. Fluids 19, 042104.
[9] Peters, I., Snoeijer, J.H., Daerr, A., Limat L. 2009, Phys. Rev. Lett. 103, 114501.
[10] Voinov, O.V. 1976, Fluid Dynamics 11, 714, and Cox, R.G. 1986, J. Fluid Mech. 168, 169.
[11] De Coninck, J., Blake, T.D. 2008, Ann. Rev. Mater. Res. 38, 1
[12] Burnett, J.H., Kaplana, S.G., Shirleya, E.L., Tompkins, P.J. and Webb, J.E. Proceedings of SPIE 5754 Optical Microlithography XVIII
[13] Riepen, M., Evangelista, F., and Donders, S. 2008, Proceedings of the 1st European Conference on Microfluidics
[14] Winkels, K.G., Peters, I.R., Evangelista, F., Riepen, M., Daerr, A., Limat, L., Snoeijer, J.H. 2011, to appear in Eur. Phys. J. Special Topics.